

74275**High-Ti Mare Basalt
1493 g, 17 x 12 x 4 cm****INTRODUCTION**

74275 is a porphyritic high-Ti basalt. It was described as a medium dark gray basalt, with a slabby to subangular shape (Apollo 17 Lunar Sample Information Catalog, 1973). The surface of the sample contains 5% vugs (up to 2cm) and vesicles (~2mm) which are irregularly distributed (Fig. 1). The vesicles are smooth and generally lined with ilmenite, whereas the vugs contain plagioclase, pyroxene, and opaques. Zap pits are abundant on T, E, N, and W, with a few on S, but none on B.

**PETROGRAPHY AND
MINERAL CHEMISTRY**

74275 is a medium-grained subophitic basalt and was described by Brown et al. (1975) as a "Type 1A." Apollo 17 basalt. 74275 contains groundmass

plagioclase, pyroxene, and ilmenite (< 0.1mm) and a high proportion of pink pyroxene (up to 0.5 mm) and olivine (up to 0.7 mm), and ilmenite (up to 0.7mm in length) (Fig. 2). Pyroxene reaction rims (~05 mm wide) are present on some olivine phenocrysts (Fig. 2). Small, euhedral chromites (< 0.05mm) are present in the olivine phenocrysts. Armalcolite forms cores (~0.1mm) to the larger ilmenite grains. Minor FeNi metal and troilite (< 0.01 mm) may or may not be associated with each other and are present either as interstitial phases or associated with ilmenite. Brown et al. (1975) reported the following modal mineralogy for 74275,32: 10.4% olivine, 25.7% opaques, 17.2% plagioclase, 45% clinopyroxene, and 1.7% silica. The whole-rock analyses (Table 1) define 74275 as a High-Ti mare basalt (8.75-12.75 wt% TiO₂).

Pyroxenes exhibit little zonation and are titan-augites (Brown et al. (1975). Sung et al. (1974) reported a range of pyroxene compositions from augite (Wo₄₄) to subcalcic augite (Wo₃₇) but are zoned with respect to TiO₂ (3.5 wt% to 6.1 wt%) and Al₂O₃ (4.2 to 7.1 wt%). Olivines are Mg-rich and range from Fo₇₁ to Fo₈₂ (Brown et al., 1975). This range of Fo contents reflects the presence of a dunitic xenolith in this sample {Walker et al., 1973; Meyer and Wilshire, 1974; Delano and Lindsley, 1982) which appears to have been entrained during magma ascent. The dunite contains olivines ranging from Fo₇₁₋₈₂, whereas 74275 contain olivines of Fo₇₀₋₇₉. Plagioclase is An-rich and exhibits little variation. Pearce and Timms (1992) used interference imaging to examine the plagioclase in 74275 and found no appreciable zoning. Composition of the chromite

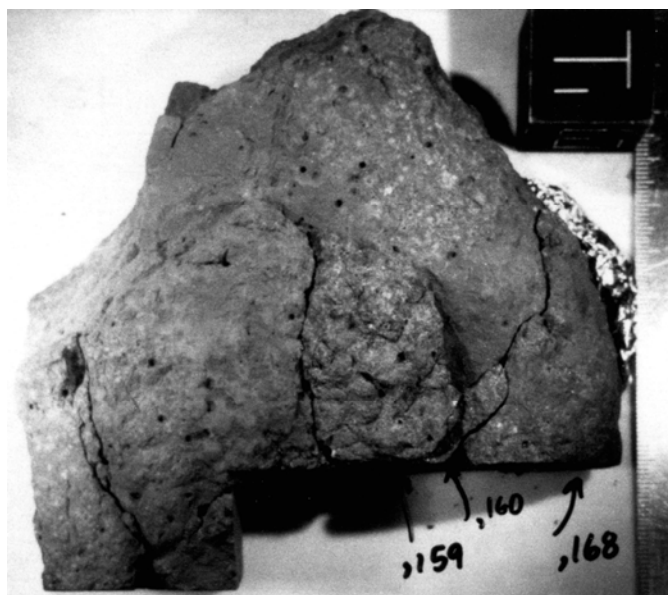


Figure 1: Hand specimen photograph of 74275,0.

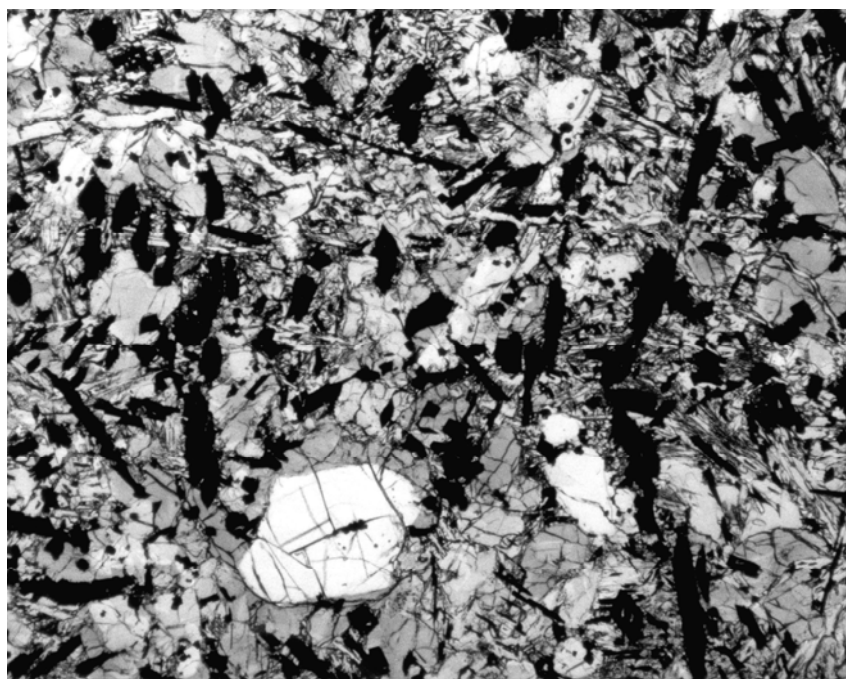


Figure 2: Photomicrograph of 74275. Field of view = 2.5 mm.

inclusions in olivine have been reported by Hodges and Kushiro (1974) as $\text{Chr}_{36-34}\text{Ulv}_{52-48}\text{Sp}+\text{Her}_{16-14}$. Study of the opaque minerals in 74275 was undertaken by El Goresy et al. (1974). Although these authors did not report specific opaque mineral analyses from 74275, they described this basalt as having a "Type II" crystallization path: Olivospinel + Olivine \rightarrow Armalcolite \rightarrow Ilmenite \rightarrow Titanaugite \rightarrow Plagioclase + Tridymite. Heiken and Vaniman (1989) used 74275 in an assessment of potential lunar resource materials and concluded that 74275 would not produce appreciable free ilmenite grains unless extensively crushed, due to the extremely fine, skeletal nature of the ilmenite.

WHOLE-ROCK CHEMISTRY

The whole-rock chemistry of 74275 has been determined using a variety of analytical

methods (e.g., Optical Emission, XRF, INA, Instrumental Thermal and Fast Neutron Activation). Six different major element compositions have been reported for 74275 and four of these also reported a number of trace element abundances (Table 1). In general, the analyses are very similar in composition, except for TiO_2 in the analysis of Miller et al. (1974) for 74275,63, which appears to be somewhat lower than other analyses and Ba for 74275,98 of Rose et al. (1974), which appears to be a little high (Table 1). Rhodes et al. (1976) defined 74275 as a Type C Apollo 17 high-Ti mare basalt on the basis of its Mg-rich chemistry ($\text{MG}\# = 50.4$). The analyses of Wanke et al. (1974) and Rhodes et al. (1976) included the REE (Fig. 3) The REE profiles again demonstrate the general similarity of each whole-rock determination. The REE abundances are almost identical, as is the magnitude of the Eu anomaly $[(\text{Eu}/\text{Eu}^*)\text{N} =$

0.50 for Rhodes et al., 1976, and 0.47 for Wanke et al., 1974). Both REE profiles are LREE depleted with a maximum at Gd (Fig. 3).

There have been several specialized studies which have concentrated upon determining only a few specific trace elements in 74275. For example, Dickinson et al. (1988, 1989) determined the Ge abundance of 74275 as 6.5 ppb (Table 1) in their study of mantle metasomatism within the Moon. Whole-rock trace-element determinations have also been reported in radiogenic (K, Ba, Rb, Sr, U, Th, Pb - Nunes et al., 1974; Murthy and Coscio, 1976; Nyquist et al., 1976) and stable (S, C, N, and H - Gibson and Moore, 1976; Gibson et al., 1975, 1976, 1987; Des Maris, 1980) isotopic studies (Table 1). Two studies (Garg and Ehmann, 1976; Hughes and Schmitt, 1985) have concentrated upon Zr/Hf ratios between chemically defined basaltic groups in order to understand lunar evolution.

RADIOGENIC ISOTOPES

Radiogenic isotope studies involving 74275 have reported Sr and Pb isotopic compositions to date. Three different Sr isotopic studies (Murthy and Coscio, 1976, 1977; Bansal et al., 1975 and Nyquist et al., 1976) have reported whole-rock isotopic ratios. Nyquist et al. (1976) reported an age for 74275, 56 of 3.83 ± 0.06 Ga (Fig. 4a), identical to another Type C basalt 74255 (see above), and Murthy and Coscio (1977) reported an age of 3.85 ± 0.08 Ga for 74275,55 (Fig. 4b). Both of these basalts have the same initial $^{87}\text{Sr}/^{86}\text{Sr}$ ratio of 0.69924 ± 3 (Table 2). Nyquist et al. (1976) reported model ages of 4.08 ± 0.19 Ga relative to BABI, and 4.29 ± 0.19 Ga relative to Apollo 16. Paces et al. (1991) used 74275 data as part of a comprehensive study of the isotopic systematics in samples from Apollo 17.

Nunes et al. (1974) reported the whole-rock Pb isotopic composition for 74275 (Table 3). This sample proved to be one of the least radiogenic lunar samples with regard to Pb (Fig. 5). Nunes et al. (1974) used this analysis of 74275 in their Pb isotopic study of lunar formation and subsequent evolution.

STABLE ISOTOPES

The S and C isotopic compositions of 74275 have been determined by Petrowski et al. (1974: C and S), Rees and Thode (1974: S only), Gibson et al. (1975: S only), and Des Maris (1980: S and C) (Table 4). The reported S^{34}S values range from -0.1‰ (Gibson et al., 1975) to $+2.0\text{‰}$ (Petrowski et al., 1974), with the $^{63}\text{S}^{34}\text{S}$ composition reported by Rees and Thode (1974) being $+0.6$. Carbon isotopes are typically light - Petrowski et al. (1974) reported

a $\text{S}^{13}\text{C}_{\text{PDB}}$ value of -28.2‰ . Des Maris (1980) demonstrated that the S^{13}C ratio became progressively heavier, as expected, with increasing temperature. The initial composition at 420°C was -30‰ .

EXPOSURE AGES AND COSMOGENIC RADIONUCLIDES

Exposure ages for 74275 have been determined by a number of different studies. Eberhardt et al. (1974; 1975) reported a $\text{Kr}^{81}\text{-Kr}$ age of 32.0 ± 1.0 Ma and a $\text{Ar}^{38}\text{-Ar}^{37}$ age 25 ± 3 Ma. The studies of Horz et al. (1975) and Goswami and Lai (1974) reported the 25 Ma exposure age of Eberhardt et al. (1974, 1975).

Cosmogenic radionuclide abundances and ratios for 74275 have been extensively analyzed. Eugster et al. (1977) reported

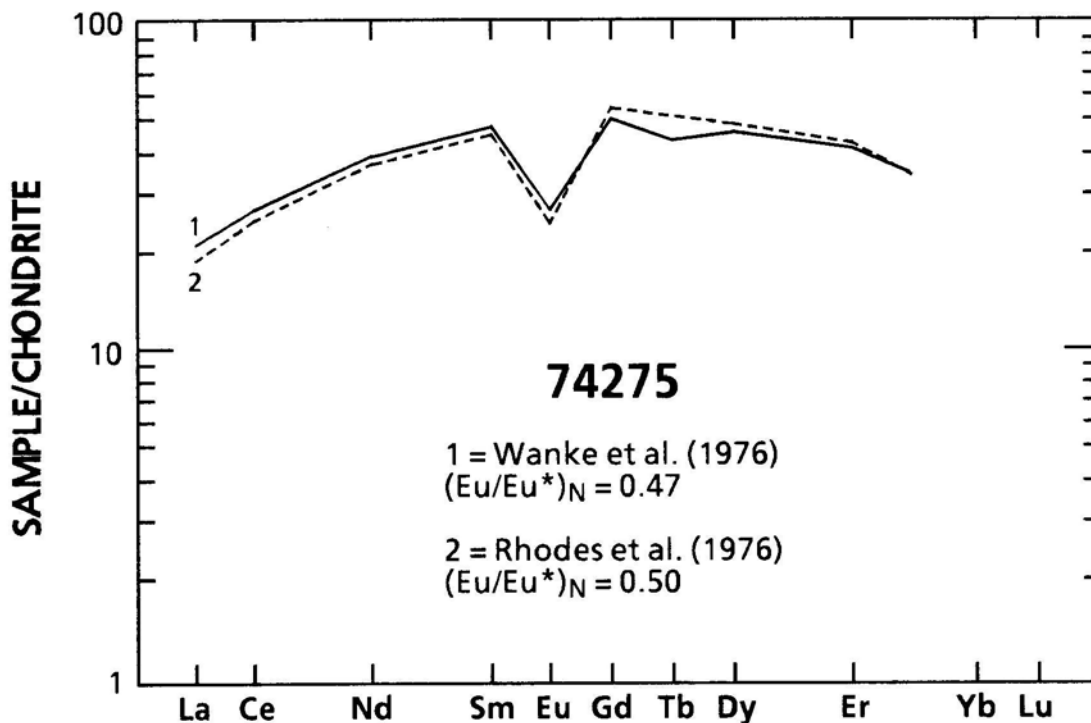


Figure 3: Chondrite-normalized rare-earth-element profiles of 74275.

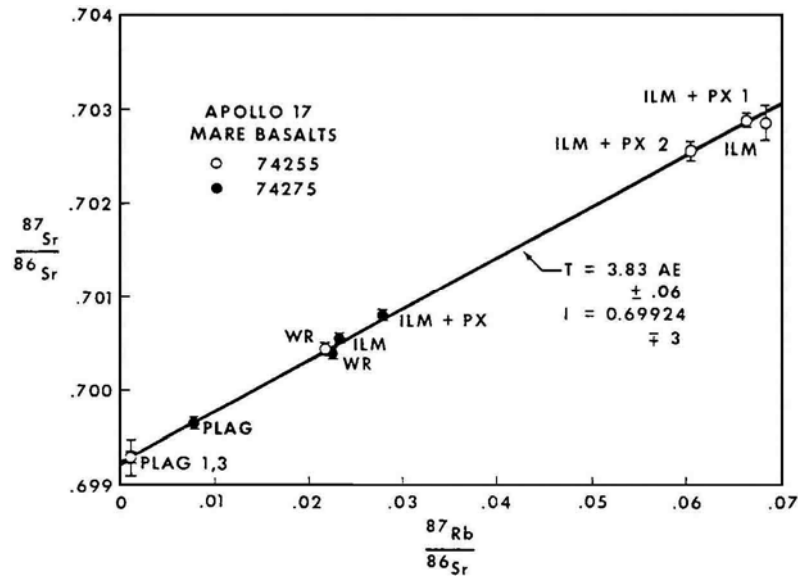


Figure 4a: Mineral separate data for 74255,25 and 74275,56. The mineral isochron shown in the figure is for 74255 data only. Uncertainties are 20 values from the York (1966) program. 74275 data are completely consistent with this isochron and independently define $I = 0.69923 \pm 0.00010$ and $T = 3.81 \pm 0.32 \text{ AE}$. After Nyquist et al. (1976).

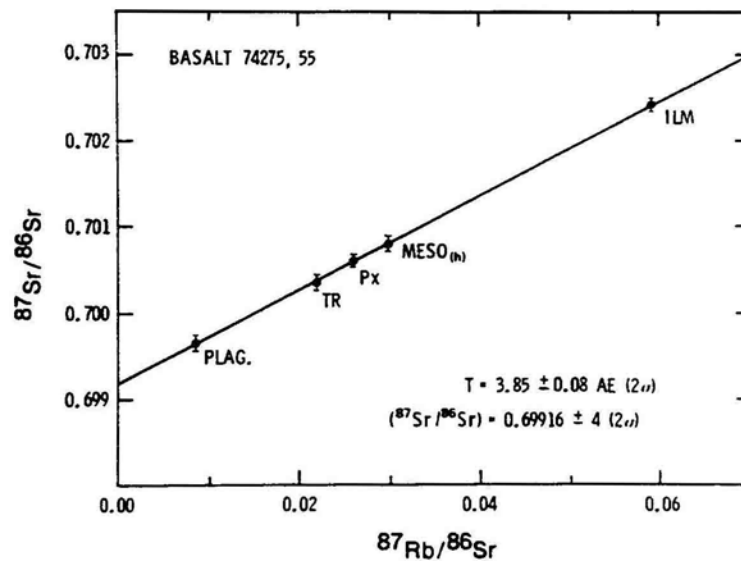


Figure 4b: Internal isochron for type C basalt 74275. T, I parameters obtained by York-regression method. Errors for the $^{87}\text{Rb}/^{86}\text{Sr}$ ratios are $\pm 2\%$. After Murthy and Coscio (1977).

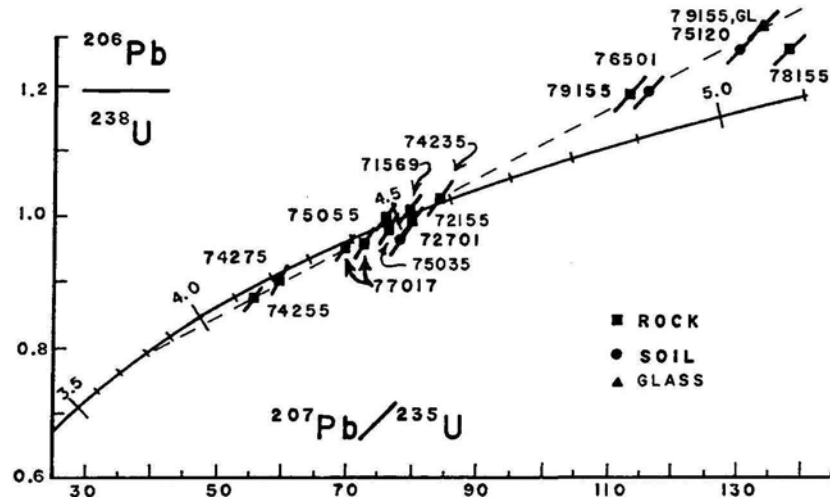


Figure 5. Concordia diagram (Wetherill, 1956). Apollo 17 mare basalts (74275, 74255, 74235, 75055, 75035, 72155, and 71569), highland rocks (77017 and 78155), soils (72701, 75120, and 76501), and a whole-rock and glass separate of 79155 are plotted. U/Pb errors are $\pm 2\%$. Data are corrected for blank and primordial lead. After Nunes et al. (1974).

He, Ne, Ar, Kr, and Xe ratios, whereas Eberhardt et al. (1975) reported Kr isotopic ratios (Table 4). Fruchter et al. (1982) analyzed 74275 at different "depth" intervals for ^{26}Al and ^{22}Na (Table 5), noting the decrease of these isotope abundances further into the sample. Klein et al. (1988) undertook a similar study, but analyzed ^{10}Be as well as ^{26}Al (Table 5). The results of these two studies for ^{26}Al are somewhat different, but the depth intervals of samples analyzed by Klein et al. (1988) are smaller than those of Fruchter et al. (1982).

MAGNETIC STUDIES

Magnetic properties of 74275 have been determined in four major studies. These studies have been undertaken to determine the $\text{Fe}^0/\text{Fe}^{2+}$ ratio (Brecher et al., 1974; Pearce et al., 1974; Nagata et al., 1975) and to demonstrate the presence of meteoritic kamacite in the

lunar regolith (Nagata et al., 1974). Results of these studies are presented in Table 6 and Fig 6 a,b.

EXPERIMENTAL

74275 has been used in a variety of experimental procedures. Green et al. (1974, 1975) reported that 74275 was multiply saturated (olivine + low-Ca pyroxene + high-Ca pyroxene) at 12-13 kbar and 1320°C . Such studies have been used to demonstrate a deep origin for the high-Ti mare basalts. The work of Green et al. (1974, 1975) also demonstrated that ilmenite could not be a residual phase after partial melting.

O'Hara and Humphries (1975), Irving et al. (1978), and Stanin and Taylor (1979) used 74275 in their studies of high-Ti basalt crystallization. O'Hara et al. (1975) studied the stability of armalcolite. These authors concluded that armalcolite

crystallizes at $\sim 1146^\circ\text{C}$ when the $f\text{O}_2$ is between $10^{-13.5}$ and $10^{-12.5}$ atm. Irving et al. (1978) used 74275 to determine REE and Sc partition coefficients between armalcolite, ilmenite, and olivine, and mare basalt melt. Results are presented in Fig. 7 a,b and Table 7. These authors noted very little difference in Kds between ilmenite and armalcolite. Stanin and Taylor (1979) used 74275 in a study of ilmenite/armalcolite textures and concluded that the $f\text{O}_2$ controls the crystallization sequence, and it is the crystallization sequence that controls the ilmenite/armalcolite textures. For example, if pyroxene crystallizes before armalcolite becomes unstable, it will armor it against reaction with the melt. Conversely, if pyroxene does not crystallize before armalcolite instability, armalcolite will have mantles of ilmenite. This was emphasized by Usselman and Lofgren (1976) who determined the temperature- $f\text{O}_2$ regime for

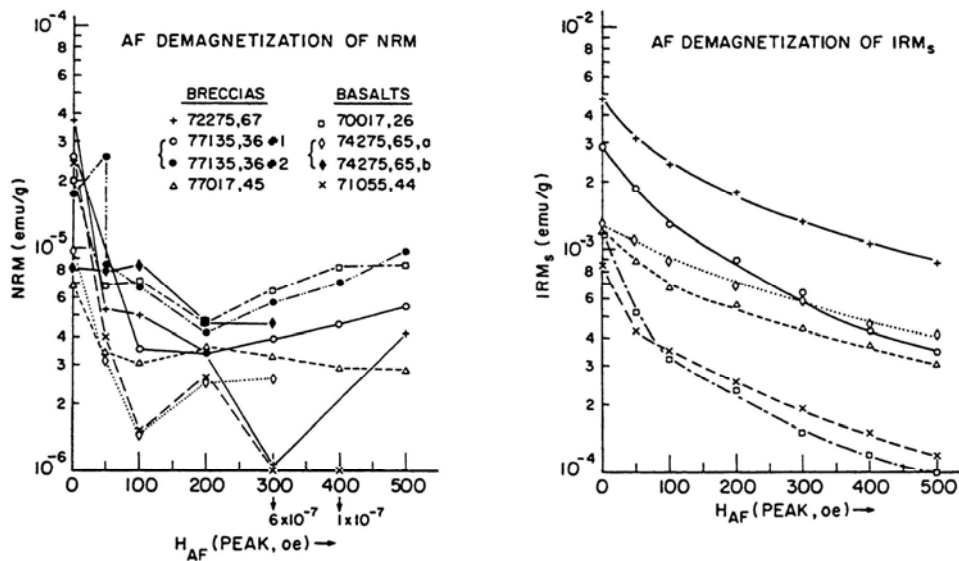


Figure 6a: The absolute AF demagnetization losses of (a) NRM and (b) saturation remanence, IRMs. A continuum of remanent behavior is apparent.

ilmenite crystallizing before and after pyroxene in 74275 (Fig. 8). Usselman et al. (1975) experimentally determined the cooling rate of 74275 as being 5-10°C/hour.

74275 has also been used in experiments to determine the Fe/Mg partitioning between olivine and liquid (Longhi et al., 1978), as well as demonstrating the heterogeneous source

regions for high-Ti basalts (Walker et al., 1976). This basalt (74275,25) has also been used in geophysical experiments to determine the compressional (V_p) and shear-wave (V_s) velocities of lunar samples (Mizutani and Osako, 1974). The P-wave velocity of 74275,25 increases from 4.14 km/sec at 0 kbar, to 7.28 km/sec at 9 kbar. The S-wave velocity was not detectable at 0 kbar, but has a

velocity of 4.11 km/sec at 9 kbar (Mizutani and Osako, 1974).

PROCESSING

74275,0 has been entirely subdivided. The largest pieces of 74275 remaining are ,2 (876g) and ,29 (159g). Seventeen thin sections are available (74275,81-,97).

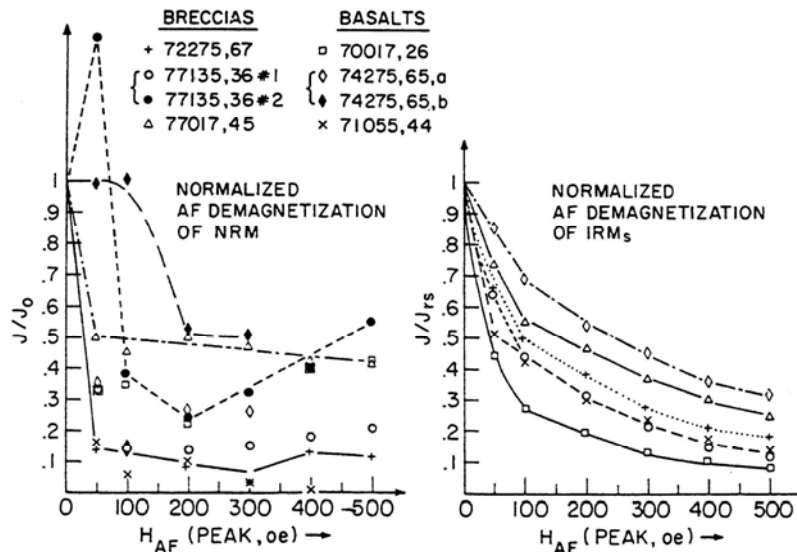


Figure 6b: Normalized demagnetization curves of (a) NRM and (b) IRM, affords a better comparison: chips of shocked basalts (74275 and 77017) display the highest stability of remanence.

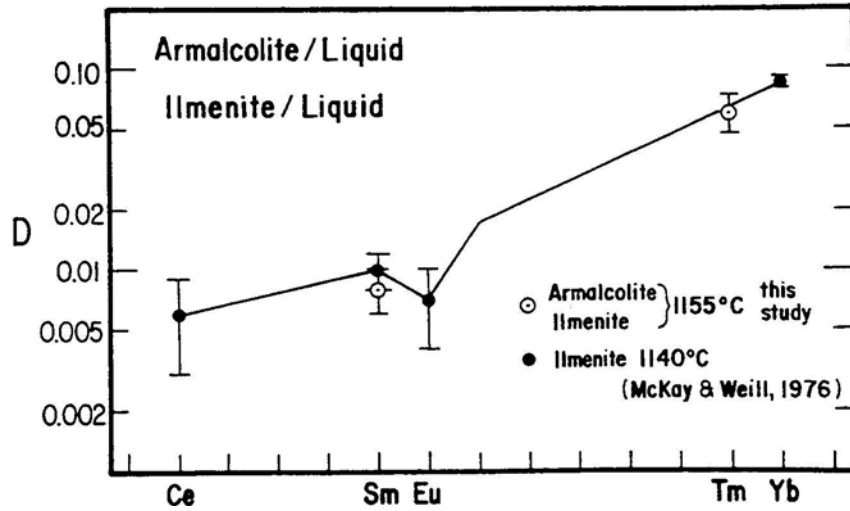


Figure 7a: Rare-earth-element partition coefficients for armalcolite and ilmenite compared with other experimental values. Ilmenite data from this study are indistinguishable from those for coexisting armalcolite.

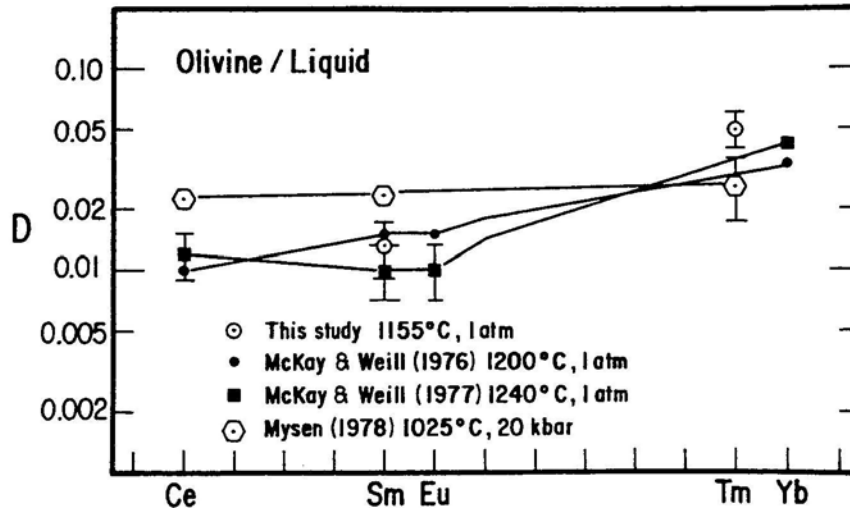


Figure 7b: Rare-earth-element partition coefficients for olivine compared with other experimental values

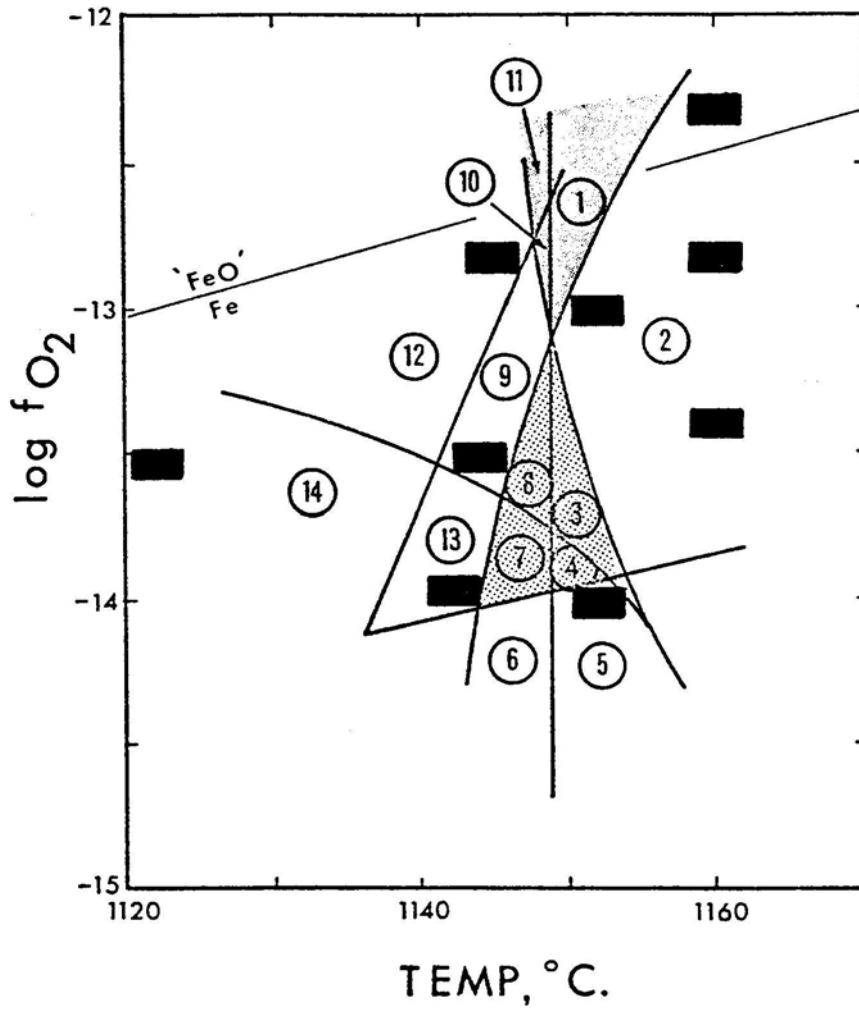


Figure 8: Phase relations of 74275 between 1120° and 1170T. The shaded region indicated the Λ regime where ilmenite crystallizes before pyroxene and the dotted region indicates the Λ regime where pyroxene crystallizes before ilmenite. The size of the boxes denote the estimated errors. Detailed phase assemblages are: (1) 11+Arm+01 +Sp+L; (2) Arm 4-01 +Sp+L; (3) Aug 4-Arm +01 +Sp 4-L; (4) Pig+Aug+Arm+Ol+Sp+L; (5) Pig+Aug+Arm+Ol+L; (6) Pl+Pig+Aug+Arm+01+L; (7) Pl+Pig+Aug+Arm+Ol+Sp+L; (8) Pl+Aug-FArm+Ol+L; (9) 11+Pl+Aug+Arm+01 +Sp+L; (10) 11 +Pl+Arm+Sp+L; (11) 11+Pl+Arm +01+L; (12) 11 +Pl+Aug+Arm+01 +L; (13) 11+Pl+Pig+Aug+Arm+01+Sp+L; and (14) 11 +Pl +Pig+Aug +Arm +01 +L. (Data from Usselman and Lofgren, 1976).

Table 1: (Concluded).

Sample Ref.	,78 1	,56 2	,98 3	,69 4	,30 5	,63 5	,54 6	,62 7	,56 8	,175 9	10	11	11	12	,56 13	,147 14
Er		9.66		9.4												
Yb		8.47	11	9.02												
Lu				1.3												
Ga			6.2	3.4												
F																
Cl											2.8					
C																7.65
N																0.2
H															3.8	
He																
Pd (ppb)				<2												
Ge				<0.1										6.8		
Re				<0.5												
Ir																
Au				0.19												
Ru																
Os																

References: 1 = Duncan et al. (1974); 2 = Rhodes et al. (1976); 3 = Rose et al. (1975); 4 = Wanke et al. (1974); 5 = Miller et al. (1974); 6 = Petrowski et al. (1976); 7 = Rees and Thode (1974); 8 = Gibson and Moore (1974, 1976); 9 = Hughes and Schmitt (1985); 10 = Jovanovic and Reed (1980); 11 = Garg and Ehmann (1976); 12 = Dickinson et al. (1988, 1989); 13 = Gibson et al. (1987); 14 = Des Maris (1980).

Table 2: Rb-Sr Isotopic Composition of 74275.

Ref. Sample Mineral	1 ,56 WR	1 ,56 WR	1 ,56 Plag	1 ,56 Ilm + Px	1 ,56 Ilm	2 ,55 WR	3 WR	3 Px	3 Meso	3 Ilm	3 Plag
Wt (mg)	62.0	15.0	2.4	49.0	7.2	20.2	20.21	21.92	3.91	13.31	11.43
K (ppm)						557	357.3				1174
Ba (ppm)						73.8	73.83				149.2
Rb (ppm)	-----	1.20	1.13	1.58	1.42	1.03	1.03	1.01	1.925	0.1795	1.279
Sr (ppm)	160	153	417	163	172	134.94	134.9	112.1	186.9	8.76	440.6
⁸⁷ Rb/ ⁸⁶ Sr	-----	0.0226	0.00783	0.0282	0.0240	0.0221	0.02208	0.02607	0.02978	0.05924	0.008394
Error	-----	±2	±9	±2	±2						
⁸⁷ Sr/ ⁸⁶ Sr	0.70041	0.70042	0.69967	0.70080	0.70055	0.70034	0.70034	0.70060	0.70079	0.70242	0.69964
Error	±6	±5	±6	±6	±8	±5	±7	±5	±9	±5	±8
T _{BABI}		4.08 ± 0.19									
T _{LUNI}		4.29 ± 0.19									

References: 1 = Nyquist et al. (1976); 2 = Murthy and Coscio (1976); 3 = Murthy and Coscio (1977).

WR = Whole-Rock; Plag = Plagioclase; Ilm = Ilmenite; Px = Pyroxene; Meso = Mesostasis.

Table 3: U-Th-Pb Isotopic Composition of 74275.
Data from Nunes et al. (1974).

	wt (mg)	U (ppm)	Th (ppm)	Pb (ppm)	$^{232}\text{Th}/^{238}\text{Th}$	$^{238}\text{U}/^{204}\text{Pb}$				
	181.0	0.1360	0.4654	0.2649	3.54	430				
	Corrected for blank & primordial Pb				Single stage ages (MA)					
Run	$^{206}\text{Pb}/^{238}\text{U}$	$^{207}\text{Pb}/^{235}\text{U}$	$^{207}\text{Pb}/^{206}\text{Pb}$	$^{208}\text{Pb}/^{232}\text{Th}$	$^{206}\text{Pb}/^{238}\text{U}$	$^{207}\text{Pb}/^{235}\text{U}$	$^{207}\text{Pb}/^{206}\text{Pb}$	$^{208}\text{Pb}/^{232}\text{Th}$		
C2P	0.9005	59.85	0.4824	0.2247	4,178	4,226	4,249	4,152		
C2	0.9017	59.71	0.4805	-----	4,182	4,224	4,244	----		
	wt (mg)	Run	Observed ratios				Corrected for analytical blank			
			$^{206}\text{Pb}/^{204}\text{Pb}$	$^{207}\text{Pb}/^{204}\text{Pb}$	$^{208}\text{Pb}/^{204}\text{Pb}$	$^{206}\text{Pb}/^{204}\text{Pb}$	$^{207}\text{Pb}/^{204}\text{Pb}$	$^{208}\text{Pb}/^{204}\text{Pb}$	$^{207}\text{Pb}/^{204}\text{Pb}$	$^{208}\text{Pb}/^{206}\text{Pb}$
105.1	P		321.7	161.1	304.7	449.9	226.6	418.3	0.4947	0.9298
109.8	C1		360.9	180.0	----	519.9	256.3	----	0.4931	----

Table 4: Exposure Ages of 74275.

Data from Eugster et al. (1977)

wt (g)	^{83}Kr (10^{-12} cm ³ STP/g)	$^{78}\text{Kr}/^{83}\text{Kr}$ x 100	$^{80}\text{Kr}/^{83}\text{Kr}$ x 100	$^{81}\text{Kr}/^{83}\text{Kr}$ x 100	$^{82}\text{Kr}/^{83}\text{Kr}$ x 100	$^{84}\text{Kr}/^{83}\text{Kr}$ x 100	$^{86}\text{Kr}/^{83}\text{Kr}$ x 100
0.728	86 ± 17	10.10 ± 0.08	33.19 ± 0.40	0.289 ± 0.007	85.6 ± 0.3	256.4 ± 2.0	70.7 ± 0.9

Data from Eugster et al. (1977)

Sample	^{86}Kr (10^{-12} cm ³ STP/g)	$^{78}\text{Kr}/^{86}\text{Kr}$ x 100	$^{80}\text{Kr}/^{86}\text{Kr}$ x 100	$^{81}\text{Kr}/^{86}\text{Kr}$ x 100	$^{82}\text{Kr}/^{86}\text{Kr}$ x 100	$^{83}\text{Kr}/^{86}\text{Kr}$ x 100	$^{84}\text{Kr}/^{86}\text{Kr}$ x 100
74275,24	61 ± 12	14.7 ± 0.7	46.75 ± 0.60	0.405 ± 0.010	121.1 ± 0.6	141.5 ± 3.0	363 ± 3

Data from Eugster et al. (1977)

Sample	^{132}Xe (10^{-12} cm ³ STP/g)	$^{124}\text{Xe}/^{132}\text{Xe}$ x 100	$^{126}\text{Xe}/^{132}\text{Xe}$ x 100	$^{128}\text{Xe}/^{132}\text{Xe}$ x 100	$^{129}\text{Xe}/^{132}\text{Xe}$ x 100	$^{130}\text{Xe}/^{132}\text{Xe}$ x 100	$^{131}\text{Xe}/^{132}\text{Xe}$ x 100	$^{134}\text{Xe}/^{132}\text{Xe}$ x 100	$^{136}\text{Xe}/^{132}\text{Xe}$ x 100
74275,24	48 ± 10	2.42 ± 0.06	3.77 ± 0.05	12.55 ± 0.20	102.2 ± 1.4	18.02 ± 0.20	100.3 ± 0.9	38.8 ± 0.7	32.8 ± 2.5

Data from Eugster et al. (1977)

Sample	wt (mg)	^4He	^{20}Ne	^{40}Ar	$^4\text{He}/^3\text{He}$	$^{20}\text{Ne}/^{22}\text{Ne}$	$^{22}\text{Ne}/^{21}\text{Ne}$	$^{36}\text{Ar}/^{38}\text{Ar}$	$^{40}\text{Ar}/^{36}\text{Ar}$
		(10 ⁻⁸ cm ³ STP/g)							
74275,24	728	8,800 ± 800	3.44 ± 0.35	1,980 ± 250	430 ± 5	0.85 ± 0.05	1.16 ± 0.02	0.693 ± 0.010	779 ± 20

Table 5: Cosmogenic Radionuclide Abundances Correlated with Depth in 74275.

Sample	Depth Range (mm)	Ave. Depth (g/cm ²)	²⁶ Al (dpm/kg)	²² Na (dpm/kg)	¹⁰ Be (dpm/kg)
74275,161@	0-10	0.9	125 ± 2	232 ± 17	
74275,162@	10-19	3.9	68 ± 3	128 ± 27	
74275,165@	19-26	6.3	58 ± 3	85 ± 21	
74275,164@	26-34	8.7	51 ± 3	73 ± 24	
74275,163@	34-44	11.1	40 ± 1	69 ± 9	
74275,197*	0-0.5	0.08			10.5 ± 0.5
74275,198*	1.0-1.5	0.42	181 ± 18		10.4 ± 0.5
74275,199*	2.0-2.5	0.76	161 ± 16		10.4 ± 0.4
74275,200*	3.0-4.0	1.18			11.2 ± 0.8
74275,201*	4.5-5.5	1.68	120 ± 12		9.8 ± 0.5
74275,202*	6.0-7.0	2.18			10.2 ± 0.5
74275,161*	7.5-9.5	2.86	84 ± 8		9.6 ± 0.4
74275,180*	0-9.5	1.6	128 ± 16		10.8 ± 1.0
74275,182*	9.5-18.5	4.7	56 ± 7		10.8 ± 1.0
74275,188*	18.5-25.5	7.4	54 ± 8		10.4 ± 0.4
74275,186*	25.5-33.5	9.9			11.0 ± 2.0
74275,184*	33.5-37.5	11.9	50 ± 6		10.4 ± 0.8
74275,190*	44.5-49.5	15.8	48 ± 5		9.6 ± 1.3

@ = data from Fruchter et al. (1982); * = data from Klein et al. (1988).

Table 6: Magnetic Data from 74275.

Reference Sub-Sample wt (g)	1 ,65A 0.617	1 ,65B 0.295	2 ,32 --	3 ,56 --	4 ,32 --
NRM ₀	0.617	0.295			
NRM* (10 ⁻⁵ emu/g)	1.1	2.6			
NRM ₁₀₀	0.147	0.84			
IRM _s (10 ⁻³ emu/g)	1.28	-			
NRM*/NRM ₀	0.87	0.31			
NRM ₁₀₀ /NRM*	0.15	1.02			
IRM _s /NRM	115	-			
I _n			4.4		
I _o			0.5		
H _o			21		
h			13		
H _o '			3		
DIV/I			0.26		
J _s (emu/g)				0.424	
X _p (emu/g Oe) x 10 ⁶				35.9	
X _o (emu/g) x 10 ⁴				0.6	
J _{rs} /J _s				0.013	
H _c (Oe)				22	
Equiv. wt% Fe ^o				0.19	
Equiv. wt% Fe ²⁺				16.5	
Fe ^o /Fe ²⁺				0.012	
I _s					0.29

**Table 7: Experimentally Determined Trace Element Partition Coefficients
between Ilmenite, Olivine, and Armalcolite using 74275.**
Data from Irving et al. (1978).

Element	Temp. (°C)	Armalcolite/Liquid	Ilmenite/Liquid	Olivine/Liquid
Sm	1157	0.008 + 0.002	0.008 + 0.002	0.013 + 0.004
Tm	1153	0.060 + 0.015	0.06 + 0.01	0.045 + 0.012
	1156	0.062 + 0.012	0.06 + 0.01	0.053 + 0.010
Sc	1156	2.2 + 0.4	---	0.75 + 0.17
Cr	1157	10	12	0.7
	1153	11	---	0.9
Mn	1157	0.3	1.2	1.1
	1153	0.3	---	1.1